

Charge ordering and inter-layer coupling in cuprates

P. Sule

Research Institute for Technical Physics and Material Science,
Konkoly Thege u. 29-33, Budapest, Hungary,
sule@mfa.kfki.hu

(January 9, 2022)

We analyze the superconducting state and c-axis charge dynamics of cuprates using a charge ordered bilayer superlattice model in which pairing is supported by inter-layer Coulomb energy gain (potential energy driven superconductivity). The superlattice nature of high- T_c superconductivity is experimentally suggested by the smallness of the in-plane coherence length $\xi_{ab} \approx 10-30 \text{ \AA}$ which is comparable with a width of a $3a_0 \times 3a_0$ to $8a_0 \times 8a_0$ ($a_0 \approx 3.9 \text{ \AA}$) square supercell lattice layer. The 2D pair-condensate can be characterized by a charge ordered state with a "checkerboard" like pattern seen by scanning tunneling microscopy. The 2D, 3D quantum phase transition of the hole-content at T_c , supported by c-axis optical measurements, is also studied. The pair condensation might lead to the sharp decrease of the normal state c-axis anisotropy of the hole content and hence to the decrease of inter-layer dielectric screening. The drop of the c-axis dielectric screening can be the primary source of the condensation energy below T_c . We find that a net gain in the electrostatic energy occurs along the c-axis, which is proportional to the measured condensation energy (U_0) and with $T_c : E_c^{3D} \approx 2N^2 U_0 / k_B T_c$ and is due to inter-layer charge complementarity (charge asymmetry of the boson condensate) where N is the real space period of the condensate. The bilayer model naturally leads to the effective mass of $m^* \approx 4m_e$ found by experiment. The static c-axis dielectric constant ϵ_c is calculated for various cuprates and compared with the available experimental data. We find correlation between T_c and the inter-layer spacing d_c and with the coherence area of the condensate. PACS numbers: 74.20.-z, 74.25.-q, 74.72.-h

I. INTRODUCTION

It is more or less generally accepted now that the conventional electron-phonon pairing mechanism cannot explain cuprate superconductivity, because as high a transition temperature as 164K (the record T_c up to now [1]) cannot be explained by the energy scale of lattice vibrations without leading to lattice instability [2]. It is already well established that much of the physics related to high-temperature superconductivity (HTSC) is in 2D nature, one of the basic questions to be answered, however, in the future is whether HTSC is a strictly 2D phenomenon or should also be described by a 3D theory.

A well known experimental fact is that the zero resistance occurs along the ab plane and the c-axis at the same critical temperature [3] suggesting that there must be inter-layer (IL) coupling involved in the mechanism which drives the system into HTSC. Another experiment, such as the intercalation on Bi2212 [4], however leads to the opposite conclusion. Intercalation of I or organic molecules, which expands the unit cell significantly along the c-axis, does not affect T_c . This finding is against IL coupling and supports low-dimensional theories. The large anisotropy of the resistivity (and of other transport properties) is again not in favour of 3D theories of HTSC [3]. Moreover, Basov et al. reported c-axis optical results and detected a small lowering of kinetic energy in the IL transport of cuprates [5]. Experiments on $\text{YBa}_2\text{Cu}_3\text{O}_{7-y}$ (YBCO) ultra-

thin artificial HTSC compounds, sandwiched between thick nonsuperconducting $\text{PbBa}_2\text{Cu}_3\text{O}_{7-y}$ (PBCO) layers [3,6] and on $(\text{BaCuO}_{2+x})_2 = (\text{CaCuO}_2)_n$ [7] indicate the continuous decrease of T_c with the decreasing number of superconducting (SC) layers. In particular the one-unit-cell thick sample of YBCO/PBCO heterostructure exhibits no HTSC with the $T_c \approx 20 \text{ K}$ [6,8]. Other heterostructures, such as the $(\text{Ba}_{0.9}\text{Nd}_{0.1}\text{CuO}_{2+x})_5 = (\text{CaCuO}_2)_2 = (\text{Ba}_{0.9}\text{Nd}_{0.1}\text{CuO}_{2+x})_5$, containing a single bilayer SC block isolated from each other by insulating blocks, were shown to have $T_c \approx 55 \text{ K}$ [9]. These findings again indicate the importance of IL coupling in high temperature superconductors. There are a couple of other findings against and supporting the 3D nature of HTSC [10-12]. Most notably the systematic dependence of the transition temperature T_c on the c-axis structure and, in particular, on the number of CuO_2 planes in multilayer blocks also strongly in favour of the 3D character of HTSC. It is therefore, a fundamental question whether at least a weak IL coupling is needed for driving the system to a superconducting (SC) state or a single CuO_2 layer is sufficient for HTSC [13].

There has been considerable effort spent on understanding HTSC within the context of IL coupling mechanism in the last decades in which c-axis energy is available as a pairing mechanism [14-17]. In other approaches the importance of IL hopping is emphasized vs. the direct IL Coulomb interaction of charged sheets [10,13]. There is another theory providing explanation for HTSC using the general framework of BCS combined with IL coupling

[18]. The so-called IL tunnelling (ILT) theory [10,13], however, is no longer considered a viable mechanism for SC in cuprates since ILT could provide no more than 1% of the condensation energy in certain cuprates [2,11,19].

Recently, optical data have been reported for Bi2212 [20], which supports the quantitative predictions of Hirsch [21], in which the carriers lower their kinetic energy upon pair formation (kinetic-energy-driven superconductors) and hence this is the largest contribution to the condensation energy. Anyhow, the role of direct IL Coulomb interaction is still not ruled out as a possible explanation for HTSC, especially if we take into account that no widely accepted theory is available until now which accounts for the apparent 3D nature of HTSC [10,11].

In this paper we propose a simple phenomenological model for explaining the 3D character of HTSC in cuprates supported by calculations. We would like to study the magnitude of direct Coulomb interaction between charge ordered square superlattice layers as a possible source of pairing interaction. Our intention is to understand HTSC within the context of an IL Coulomb-mediated mechanism. Of particular relevance to our investigation are the doping, multilayer, and pressure dependence of T_c in terms of a charge ordered superlattice nature of pair condensation, which is often neglected in the past.

On the other hand the size of a characteristic superlattice can directly be related to the in-plane coherence length λ_{ab} of cuprates, which is proportional to the linear size of the pair condensate (real space pairing) in the ab-plane [22]. The relevant length scale for superconductors is the characteristic size of the Cooper-pair and can be estimated by an uncertainty-principle argument [22]. Only those charge carriers play a decisive role in HTSC which has energy within $k_B T_c$ of the Fermi energy and sets in at T_c with the momentum range $p \sim k_B T_c = v_F$, where v_F is the Fermi velocity, leading to the definition of the Pippard's characteristic length [22]

$$\lambda_{ab} = a \frac{h v_F}{k_B T_c} \quad (1)$$

where a is a numerical constant of order unity, to be determined. λ_{ab} is a relevant number for describing the 2D confinement of the pair-condensate wave function below T_c . λ_{ab} can directly be obtained according to the anisotropic Ginsburg-Landau theory via the measurement of the upper critical field $H_{c2,ab}$ [22].

The IL charging energy we wish to calculate depends then on the IL spacing (d), the IL dielectric constant ϵ_c , the hole content p and the size of the superlattice. A large body of experimental data are collected which support our model. A consistent picture is emerged on the basis of the careful analysis of this data set. Finally we calculate the static c-axis dielectric constant ϵ_c for various cuprates which are compared with the available experimental observations.

It is commonly accepted that charge carriers are mainly confined to the 2D CuO_2 layers and their concentration is strongly influenced by the doping agent via hole doping. Holes (no charge and spin at a lattice site) in the 2D CuO_2 layers are the key superconducting elements in high temperature superconductivity (HTSC). A characteristic feature of many high temperature superconductors (HTSCs) is the optimal hole content value of $p_0 = 0.16$ per CuO_2 layer at optimal doping measured in the normal state (NS) [23]. This general feature of cuprates can be summarized in the parabolic dependence of maximum critical temperature T_c^m ,

$$T_c = T_c^m = 1 - 82.6(p - p_0)^2; \quad (2)$$

where T_c^m corresponds to the optimal hole concentration p_0 [24]. Since T_c appears to be maximized at $p_0 = 0.16$, we pay special attention to the IL Coulomb interaction in cuprates at this particular hole concentration.

Our starting hypothesis is that the hole content goes through a reversible 2D \leftrightarrow 3D quantum phase transition at T_c in layered copper oxides. Optical studies on the c-axis charge dynamics reveals this phenomenon: the c-axis resistance is nearly insulating in the NS but below T_c is dominated by the Josephson-like plasma edge [5]. Below T_c a sharp reactivity edge is found at very low frequencies (lower than the superconducting gap) for a variety of cuprates arising from the carriers condensed in the SC state to the ab-plane and from the onset of coherent charge transport along the c-axis [25-29]. The appearance of plasma in the SC state and the absence of it in the NS seem to be a common feature of HTSC cuprates [28]. Band structure calculations predict an appreciable c-axis dispersion of bands close to the Fermi surface and thus an anisotropic three-dimensional metallic state [30]. Other first principles calculations indicate that above T_c the hole charge p is charge transferred to the doping site (2D \rightarrow 3D transition) [31,32]. Furthermore, we expect that below T_c the hole-content condenses to the sheets forming anti-hole regions (hole-content charge at a lattice site, 3D \rightarrow 2D transition). An anti-hole corresponds to an excess charge condensed to a hole lattice site in the sheet below T_c . Therefore, in the normal state hole doping is the dominant charge transfer mechanism while in the superconducting (SC) state the opposite is true: the IL hole-charge is transferred back to the CuO_2 planes (charging of the sheets). The latter mechanism can be seen by the measurement of transport properties as a function of temperature [3,33-35] if we assume that the increase in the density of in-plane free carriers below T_c is due to pair condensation. The sharp temperature dependence of the c-axis dielectric constant ϵ_c and optical conductivity [36] seen in many cuprates and in other perovskite materials also raises the possibility of a 2D \leftrightarrow 3D charge density condensation mechanism at T_c [3,38]. Therefore, the pair condensation can be described by an anisotropic 3D condensation mechanism, and by a doping induced 2D-3D dimensional crossover [12].

In any naive model of electron pairing in cuprates the Coulomb repulsion is troublesome. When the pairs of charged carriers are confined to the 2D sheets, naturally a net self-repulsion of the pair condensate occurs. Although short-range Coulomb screening in the dielectric crystal can reduce the magnitude of the repulsion but it is insufficient to cancel Coulomb repulsion [39]. Spatial separation should reduce the interaction strength, but even at 14\AA $e^2/r \approx 1\text{eV}$ if unscreened. One can assume capacitive effect between the CuO_2 planes: The charged boson condensate in one plane is stabilized by a deficiency of that charge on another plane [39]. The various forms of the capacitor model are associated with the 3D character of HTSC, considering the inter-layer charge reservoir as a dielectric medium [39]. The inter-layer charging energy might be insufficient to stabilize the self-repulsion of the holes in one plane and the self-repulsion of the charge condensate on another plane in the capacitor model. Also, the superconducting properties of the hole-rich and nearly hole-free sheets would be different which is not verified by experimental techniques.

Our intention is to combine the 2D and 3D nature of HTSC. Therefore, we propose a phenomenological model in which the charge distribution of the planes is polarized in such a way that holes and anti-holes (hole-electron pair) are phase separated within each of the sheets leading to a charge ordered state (COS). Recently, signatures of charge ordering have been found in various cuprates and manganites in the presence and the absence of magnetic fields [41-44]. Furthermore, the "checkerboard" charge pattern seen in $\text{Bi}_2\text{Te}_2\text{O}_7$ [41] with spin periodicity of $8a_0$ strengthens our expectation that the SC state can be characterized by a COS. We focus on, then the magnitude of IL coupling (direct IL Coulomb interaction) between 2D static charge ordered superlattices.

Charging of the sheets: The CuO_2 layers carry negative charge obtained from the charge reservoir even in the insulating stoichiometric materials, e.g. in the infinite layer compound CaCuO_2 each layer is charged by $2e$ charge donated by the Ca atoms. In $(\text{CuO}_2)^2$ then the electron configuration of Cu and O is $3d^0 4s^1$ and $2p_2^2$. Unit $(\text{CuO}_2)^2$ is typical of any undoped (stoichiometric) cuprates and ab initio calculations provide approximately the charge state $\text{Cu}^{1.5+} \text{O}_2^{3.5-}$ [3,30] which is due to charge redistribution between Cu and O. The $(\text{CuO}_2)^2$ plane itself is antiferromagnetic and insulating, e.g. there are no holes in the "overcharged" layers. Upon e.g. oxygen doping, however, the doping charge p is transferred along the c -axis to the doping site, since the doping atom exhibits a rare gas electron structure (O^{2-}) [31,32].

Our basic assumption is that in the SC state every second hole with the charge of $+p$ is filled up by the doping charge p due to the condensation of the hole-content p to the sheets. Briefly, the c -axis anisotropy of the hole content is strongly temperature dependent in cuprates. The phase separation of the holes and anti-holes (leading to a charge ordered state) is stabilized by the intra-

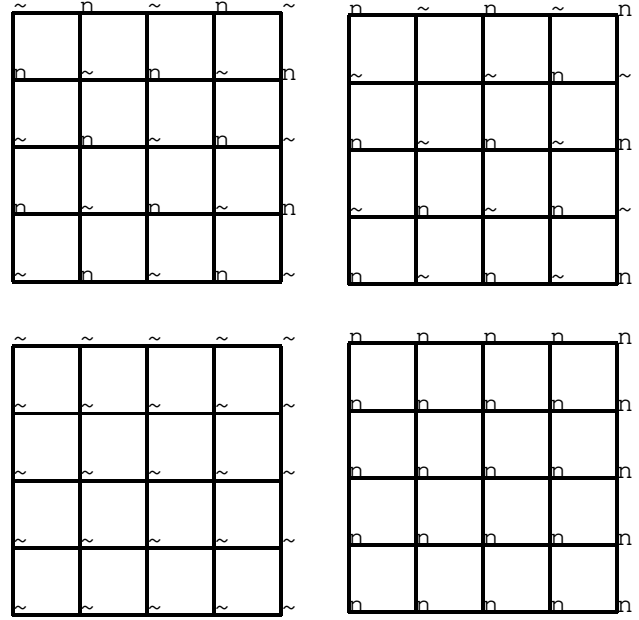


FIG. 1. Upper panels: The charge ordered state of the type of a "checkerboard" of the hole-anti-hole condensate. Open and filled circles denote the holes with a charge of $q_i = +0.16e$ and anti-holes ($q_j = -0.16e$), respectively in the $4a_0 \times 4a_0$ (5×5) square lattice layer model. Note that the left panel accommodates 13 anti-holes which corresponds to $2e + 0.16e$ charge. The right panel contains 12 anti-holes corresponding to $2e - 0.16e$ charge. The two lower panels correspond to the antiferromagnetic insulating state (left) and to the hole-doped system (normal state, right).

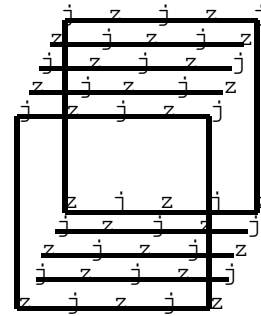


FIG. 2. The charge ordered state of the hole-anti-hole condensate in the bilayer-hole $4a_0 \times 4a_0$ superlattice model. Note the charge asymmetry between the adjacent layers. The bilayer can accommodate a pair of boson condensate ($4e$). Note-worthy that holes (empty circles) and anti-holes (filled circles) can be characterized by stripes along the diagonal lines.

and inter-layer hole-anti-hole interactions. Basically the phase separation of holes and antiholes in the planes is the manifestation of strong Coulomb correlation in the SC state. The superconducting charge-ordered states in cuprates are characterized theoretically based on the assumption that cuprates are in close proximity to quantum critical points where spin/or static charge order occurs in the SC state [45]. In this paper we will focus on the Coulomb interaction between the charge ordered sheets screened by the IL dielectric media (charge reservoir). It will be immediately apparent from our analysis that net energy gain occurs from the IL Coulomb interaction of charge ordered states when the hole-electron charge pattern is asymmetrically distributed in the adjacent layers (Fig. 2).

II. THE SUPERLATTICE MODEL

We propose to examine the following superlattice model of pair condensation: A pair of charge carriers ($2e$) is distributed over $2 \times 0.16 = 12.5$ CuO_2 unit cells in a square lattice layer if the $2e$ pair is composed of the hole charge $p = 0.16 = \text{CuO}_2$. However, allowing the phase separation of hole-anti-hole pairs, every second unit cell is occupied by $0.16e$ (antihole), and the rest is empty (holes, $+0.16e$), therefore we have 25 unit cells for a condensed pair of charge carriers (Fig. 1., that is the unit lattice of the pair condensate in the 5×5 supercell model). Therefore, $2p_0 = 0.32e$ hole charge condenses to every second hole forming antihole sites. The remarkable feature is that the size of the 5×5 condensate (four lattice spacings, $4a_0 = 15.5\text{\AA}$) is comparable with the measured small coherence length ξ_{ab} of single-layer cuprates ($\xi_{ab} = 10\text{\AA}$ to 20\AA) [3,22,44,47]. ξ_{ab} can directly be related to the characteristic size of the wave-pocket of the local Cooper pair (coherence area) [3,22]. The supercell model can be applied not only for $p_0 = 0.16e$ but also for the entire doping regime. Our expectation is that the COS of the 5×5 model given in Fig. 1 can be an effective model state for describing the SC state. An important feature of this model is the charge separation dq in the charge ordered state, where $+0.16e$ and $-0.16e$ partial boson charges are localized alternatively ($dq = 0.32e$). The hopping of charge carriers from the antihole sites to the holes can reduce the magnitude of the charge separation dq leading to the extreme case when $dq = 0$ which is nothing else than the $(\text{CuO}_2)^2$ antiferromagnetic insulating state. Therefore characteristic quantity of the SC state dq is directly related to the hole-content seen in cuprates in the NS as a function of doping.

The hopping of antiholes in such a charge ordered lattice layer might lead to SC without considering any lattice vibration effects when dq is in the optimal regime. The freezing of the COS leads to insulating Wigner crystal (the NS) [40]. Therefore the melting of the crystalized COS is required for SC [45]. HTSC can be char-

acterized in this way as a competition between liquid-crystal-like striped COS (SC) and Wigner-crystal-like phases (NS) in a semiclassical theory of hole dynamics [40].

Below T_c the charged-ordered state becomes stable compared with the competing phase of the NS supported by IL charging energy. Holes and antiholes are placed in such a way in adjacent layers to maximize IL charging energy. Therefore, holes in one of the layers are always covered by antiholes in the other layer and vice versa (Fig. 2, inter-layer electrostatic complementarity, bilayer $5 \times 5 (4a_0 \times 4a_0)$ model). An important feature is then that the boson condensate can be described by an inter-layer charge asymmetry. The IL coupling of boson-boson pairs in the bilayer 5×5 model naturally suggests the effective mass of charge carriers $m = 4m_e$, as it was found by measurements [48,51]. In the next section we generalize the 5×5 model to represent a real space periodicity of $N \times N$ coherence area. The charge ordered state presented in this article can also be studied as a charge density wave (CDW) condensed on a superlattice. Using the CDW terminology one has approximately two CDWs within a characteristic bilayer with an amplitude of $0.16e$. This system might not be insulating if we assume high rate of intersite hopping and low rate of IL hopping of the charge carriers. Then the charge ordered state is stabilized due to the attractive IL Coulomb interactions of asymmetrically condensed neighbouring CDWs.

We characterize the purely hole-doped NS as follows: In each sheet each CuO_2 unit possesses $p = +0.16e$ charge. The hole charge p is charge transferred to the charge reservoir (doping site) above T_c . In this model one can naively expect that the self-repulsion of a hole rich sheet can be quite large. In order to reduce the hole-hole self-repulsion of the sheets, a hopping of p charge between the adjacent hole sites would result in the reduction of the repulsion leading to a Wigner-crystal-like COS depicted on Fig. 3. As is well known, the hopping of certain amount of charge (p) between the holes leads to metallic conductance which is typical of hole-doped cuprates. This is the normal state (NS) of the cuprates. Due to the strong c -axis anisotropy of the hole charge in the NS IL dielectric screening is large in this state because of the increase in the dynamic component of the IL dielectric permittivity (ϵ_c) and therefore the IL interaction energy vanishes, $E_c^{NS} = 0$.

Our proposal is to understand HTSC in such a way that the pair-condensate is stabilized at higher temperature by the IL-charging energy provided by the antisymmetry of the pair-condensate charge density between the adjacent layers.

The c -axis dielectric constant of the SC state is reduced to the average value of the IL dielectric medium due to the pair condensation of the hole charge to the sheets. No IL screening of the hole charge occurs in this state which may well lead to energy gain. When the system goes to SC state, the conduction band loses its 3D anisotropy

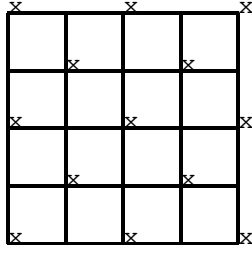


FIG. 3. The charge ordered state of the normal state. Opened and filled circles denote the holes with a charge of $q_h = +0.32e$ and antiholes ($q_j = -0.16e$), respectively in the 5×5 square lattice layer model.

due to the 2D pair-condensation of the hole-content.

III. THE TOTAL ENERGY OF THE PAIR CONDENSATE

Our intention is to develop a simple working hypothesis in which the IL charge reservoir provides an average dielectric background and the hole content further enhances IL dielectric screening when 2D \rightarrow 3D transition occurs (hole-doping, the NS). The dielectric plasma provided by the hole charge results in the dynamic screening effect of Coulomb interaction which is typical of hole doped cuprates in the NS. In the opposite case (3D \rightarrow 2D, pair condensation) the IL dielectric screening is nearly reduced to the average background value of the IL ion core spacer. This is what leads to IL energy gain. The underlying source of the condensation energy is then the energy gain due to the lack of dynamic screening in the SC state. The possibility of direct IL hopping of Cooper pairs is not considered within this model as it was ruled out as important aspect of HTSC [11].

We start from a very general description of our model system using e.g. a Hamiltonian similar to that is given elsewhere [15] or which can also partly be seen in general text books [56]. We would like to describe then the 2D \rightarrow 3D condensation of the hole-content using the Hamiltonian

$$H = \sum_i H_i^{2D} + \sum_{ij} H_{ij}^{3D}; \quad (3)$$

where H_i^{2D} is the BCS-type Hamiltonian of the intra-layer condensate.

$$H_i^{2D} = \sum_k c_{k,i}^\dagger c_{k,i} + V \sum_{k,jk^0} c_{k,i}^\dagger c_{k\#,i} c_{k\#,i} c_{k,j}; \quad (4)$$

In Eq. (4) $c_{k,i}^\dagger$ is the creation operator for electrons in the i th layer, with linear momentum k within the

layer and spin \uparrow, \downarrow , using the effective-mass approximation $\epsilon_k = \hbar^2 k^2 / 2m$. $V = -\gamma / j$ is the attractive inter-layer interaction (3D coupling) and is assumed to originate from some of the proposed mechanisms [10,14{16]. The attractive IL term H_{ij}^{3D} given by

$$H_{ij}^{3D} = t \sum_{k,j} c_{k,i}^\dagger c_{k,j} + Y \sum_{k,jk^0} c_{k,i}^\dagger c_{k,j} c_{k,j} c_{k,i} + W \sum_{k,jk^0} c_{k,i}^\dagger c_{k,j} c_{k,j} c_{k,i}; \quad (5)$$

The first term in Eq. (5) is the direct IL hopping, while the second and third terms describe IL coupling in a general form. t is very small in oxide superconductors [11,15]. Y denotes the IL coupling assisted by direct Coulomb interaction between charged layers (this is of particular interest in our model). W is the coupling constant and can arise through the Coulomb interaction causing inter-band transitions at the Fermi surface to some of the occupied or empty bands away from the Fermi level, with finite dispersion, however, along the c -axis. In this paper we consider only the second term in Eq. (5) as the source of the attractive interaction for pairing and neglect the rest of the inter-layer Hamiltonian H_{ij}^{3D} ($t = 0; W = 0$).

We calculate then the energy of the nearly 2D electron pair condensate in the CuO_2 plane for the bilayer supercell problem. It is assumed that the pair condensate behaves as a nearly free electron gas with ab-kinetic energy E_{kin}^{ab} and potential energy, which is mainly its in-plane self-electrostatic energy (E_c^{ab}) and the out-of-plane inter-layer interaction energy E_c^{IL} . For simplicity, the rest of the electron system is neglected completely. The external potential of the condensate is also excluded in this model, that is the lattice-condensate interaction, which is assumed to be negligible in the charged $(\text{CuO}_2)^2$ system (at least its contribution is negligible to the condensation energy). In other words the ionic background of the planes is screened by the core and valence electrons of the $(\text{CuO}_2)^2$ plane. The kinetic energy of the charge condensate is due to the hopping of the charge carriers between the CuO_2 sites within the sheets. We do not take into account the complications due to ionic heterogeneity, nonpointlike polarization, etc. The effective Coulomb interaction between spinless point-charges may be approximated by the expression $V_{eff}(r) = e^2 / (4 \epsilon_0 \epsilon_c r)$, where ϵ_c takes into account phenomenologically the dielectric screening effect of the IL dielectric medium and confined hole charge. This kind of a rough approximation has widely used by several groups in the last decade [14,39,48,65]. The important feature is that the c -axis dielectric screening (ϵ_c) is nearly reduced to the static value of the average background dielectric constant in the SC state. In accordance with this a sharp temperature dependence of $\epsilon_c(T)$ is found in BSCCO by c -axis optical measurements at T_c [36]. The static out-of-plane dielectric function can be obtained from the sum rule

$$\epsilon_c = \epsilon_1(0) + \frac{2}{\epsilon_0} \sum_{\mathbf{l}} \frac{2(l^0)^2}{l^0} d(l^0); \quad (6)$$

where $2(l^0)$ is the dynamic component of $\epsilon_c(l^0)$ [63].

Although, the r -dependence of the screened in-plane electrostatic interaction between the condensed charges q_i and q_j is not perfectly $1/r$, we approximate it with the expression $V_{\text{eff}}^{\text{ab}} = e^2 / \epsilon_{\text{ab}} r$ as well, where screening is taken into account implicitly via ϵ_{ab} . The lowest eigenvalue of H given in Eq. (3) is $E = \hbar^2 \mathbf{k}^2 / 2m$, where $(r_1; r_2) = \sum_{\mathbf{k}} g(\mathbf{k}) e^{i\mathbf{k} \cdot \mathbf{r}_1} e^{i\mathbf{k} \cdot \mathbf{r}_2}$ being the wavefunction of the interacting pair and $g(\mathbf{k})$ is a pair-correlation function [22]. Then the energy of the lowest eigenstate of the condensate in the SC state is approximated by using a pure dielectric form for the potential energy

$$E_{\text{tot}} = E_{\text{kin}}^{\text{ab}} + E_c^{\text{ab}} + E_c^{\text{IL}} = \frac{\hbar^2}{2m} (\mathbf{r}_1; \mathbf{r}_2) + \frac{e^2}{4\epsilon_0} \frac{1}{\epsilon_{\text{ab}}} \sum_{i,j} \frac{q_i^{(1)} q_j^{(1)}}{r_{ij}^{(1)}} + \frac{1}{\epsilon_c} \sum_{n=1}^{\infty} \sum_{m=2}^{\infty} \sum_{i,j} \frac{q_i^{(n)} q_j^{(m)}}{r_{ij}^{(nm)}}; \quad (7)$$

where \hbar is the Planck constant, $m = 4m_e$ is the effective mass for the holes induced in the half-filled bands [48], n, m are layer indices, $r_{ij}^{(1)}$ and $r_{ij}^{(nm)}$ are the intra-layer and inter-layer point charge distances, respectively. The most important components are the interactions with $r_{ij}^{(1,2)}$ (bilayer components), however one has to sum up for the IL interactions with terms $r_{ij}^{(nm)}$, where $m = [2; 1]$. Note that only the interactions of various layers with the baselbilayer (FIG. 2) are considered along the c -axis in both directions (up and down). The in-plane electrostatic screening ϵ_{ab} is completely separated from the out-of-plane dielectric screening (ϵ_c). q_i, q_j are the partial point charges/atoms in the $N \times N$ superlattice model at optimal doping.

$$q_{i,j} = \frac{2N_h}{3N^2} e; \quad (8)$$

where factor 2 is due to the fact that every second CuO_2 site is occupied by antiholes, and each of them consists of 3 atoms ($q_{i,j} = 0.53e$ at maximal charge separation). For the sake of simplicity it is assumed that the charges are equally distributed among Cu and O atoms within a CuO_2 site. The number of the lattice sites in the characteristic superlattice is N^2 and

$$\epsilon_{\text{ab}} = (N - 1)a_0 \quad (9)$$

where $a_0 = 3.88\text{\AA}$ is the ab lattice constant. $N_h = 2e$ is the charge of the electron pair. The antihole charges q_i^{ahole} must satisfy the charge sum rule within a characteristic bilayer over a coherence area $\frac{2}{\epsilon_{\text{ab}}}$

$$\sum_{i=1}^{N^2} q_i^{\text{ahole}} = 4e; \quad (10)$$

where q_i^{ahole} represents the antihole point charges. Naturally the charge neutrality $\sum_{i,j}^{N^2} (q_i^{\text{hole}} + q_j^{\text{ahole}}) = 0$ is also required. In this paper we study the lattice size $N \times N = 5$, which we found nearly optimal for a variety of cuprates. However, it can be interesting to study the variation of the "characteristic" lattice size in different cuprates as a function of various parameters (doping, pressure etc.). The kinetic energy of the boson condensate arises from the hopping of antiholes (hole-antihole exchange) between the adjacent sites within the sheets, against the electrostatic background of the rest of the hole-antihole system. Single hole-antihole exchange is forbidden since extraordinary repulsion occurs which leads to the redistribution of the entire hole-antihole charge pattern. The collective intersite antihole hopping results in the kinetic energy of the condensate. If we chose appropriately the in-plane dielectric constant [20,58]), we get the following result:

$$E_{\text{kin}}^{\text{ab}} + E_c^{\text{ab}} = 0; \quad (11)$$

Consequently, no net in-plane energy gain is available for HTSC in this model. In other words we expect no role of pairing induced kinetic energy gain contrary to other theories [2,10,21] since the kinetic energy of the condensate is cancelled by the in-plane electrostatic energy. This is basically the manifestation of the virial theorem ($2T + V = 0$) for the ab-plane and is reasonable to expect its validity when weak IL coupling is assumed, where $E_{\text{kin}}^{\text{ab}} = 2T$ and $E_c^{\text{ab}} = V$. If the inter-sheet coupling is not that weak, then kinetic energy gain can occur in the planes (the violation of the in-plane virial theorem). It can therefore be the subject of further studies that both ab-plane kinetic energy and the screened c -axis IL Coulomb interaction can be the source of the condensation energy in the SC state.

IV. THE CONDENSATION ENERGY IN THE CHARGE ORDERED BILAYER-HOLE MODEL

Important consequence of the model outlined in this paper is that the condensation energy (E_{cond}) of the SC state can be calculated. Within our model the primary source of E_{cond} is the net energy gain in IL Coulomb energy occurs due to the asymmetrical distribution of the condensed hole-charge in the adjacent layers (see Fig. 2) below T_c .

Per definition E_{cond} is the free energy difference of the normal state and the superconducting state [11]. Therefore, taking the energy difference $E_{\text{tot}} = E_{\text{tot}}^{\text{NS}} - E_{\text{tot}}^{\text{SC}}$, using Eq. (7) and dropping the terms coming from the ab-plane according to Eq. (11), the IL energy gain in the SC state (condensation energy) can be given as follows,

$$E_{\text{cond}} = E_c^{\text{IL,NS}} - E_c^{\text{IL,SC}}; \quad (12)$$

We can further simplify Eq. (12) if the NS contribution to Eq. (12) is $E_c^{\text{IL,NS}} = 0$, which holds if IL coupling is screened effectively in the NS (large density of the hole content in the IL space, large $c(\text{NS})$). Then we have

$$2N^2U_0 = E_{\text{cond}} = E_c^{\text{IL,SC}}; \quad (13)$$

where $E_c^{\text{IL,SC}}$ is the Coulomb energy gain in the SC state. U_0 is the experimental condensation energy given per unit cell. E_{cond} is the condensation energy of the bilayer system with $2N^2$ unit cells.

The energy gain in the SC state is provided by the change in the inter-layer charging energy which is essentially the change of the out-of-plane hole-antihole interaction energy below T_c . The hole-conductivity in the SC state is strictly 2D phenomenon, no direct IL hopping of quasiparticles is considered within this model. T_c is mainly determined by the inter-plane distance and by the static c-axis dielectric constant (the c-axis component of the dielectric tensor). An interesting feature of the $N \times N$ bilayer model is then that it is capable of retaining the 2D character of superconductivity while T_c is enhanced by 3D Coulomb interactions.

V. THE CONDENSATION ENERGY AND T_c

There are number of evidences are available which suggest that HTSC occurs beyond the BCS limit. In those materials which contain nearly isolated single layers, such as $\text{Bi}_2\text{Ba}_2\text{CuO}_{6+x}$ ($T_c = 20 \text{ K}$ [64]) or superlattice structures (periodic artificially layered materials) such as $\text{O-doped } (\text{BaCuO}_2)_2 = (\text{CaCuO}_2)_n$ thin films, when $n = 1$ [7] and in $\text{YBa}_2\text{Cu}_3\text{O}_{7-x} = \text{PrBa}_2\text{Cu}_3\text{O}_7$ (YBCO/PBCO) [3,6,8] the critical temperature is limited to $T_c \approx 30 \text{ K}$ (below the BCS limit), therefore these materials are not considered as high- T_c superconductors in this article. In these compounds the IL distance is so large that the CuO_2 planes are decoupled and the superconducting properties can be understood within the BCS formalism. However, the multilayer Bi-compounds (with the same charge reservoir), the $(\text{BaCuO}_2)_2 = (\text{CaCuO}_2)_n$ thin films, when $n \geq 2$ [7] or YBCO with thin $\text{PrBa}_2\text{Cu}_3\text{O}_7$ layer [3,6,8] exhibit HTSC. Therefore it is worth to explain the enhancement of T_c beyond the BCS limit assuming other mechanism than the electron-phonon coupling. Inter-layer Coulomb coupling can be a natural source of the condensation energy and of HTSC.

Checkerboard-like charge pattern (COS) seen experimentally [41-43] directly leads to IL energy gain and to potential energy driven condensation energy if the hole-antihole charge pattern is asymmetrically condensed to the adjacent layers (Fig 2). Assuming that thermal equilibrium occurs at T_c for the competing charge ordered phases of the NS and the SC state the following

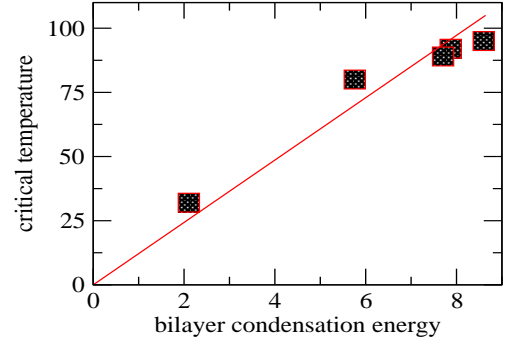


FIG. 4. The critical temperature (K) as a function of the bilayer condensation energy ($2N^2U_0$, meV) using Eq. (14). The real space period N is directly related to a_{ab} via Eq. (9). The straight line is a linear fit to the data.

equation for the condensation energy can be formulated using Eq. (13),

$$2N^2U_0 = 2 \left(\frac{a_{\text{ab}}}{a_0} + 1 \right)^2 U_0 = k_B T_c = E_c^{\text{IL,SC}}; \quad (14)$$

At a first look this formula seems to be unusual because of the dependence of the condensation energy on T_c . The available measurements of the condensation energy on various cuprates show no correlation of U_0 with the critical temperature. One of the important goals of this paper, however, to show that correlation can indeed be found with T_c if $2N^2U_0$ (the bilayer condensation energy) compared with T_c . In other words the condensation energy of the coherence bilayer-hole system shows correlation with T_c . In order to test the validity of Eq. (14) we estimate the real-space period of the pair condensate using Eqs. (14) and (9),

$$N = \sqrt{\frac{k_B T_c}{2U_0}} \left(\frac{a_{\text{ab}}}{a_0} + 1 \right); \quad (15)$$

The results are given in Table I. N can directly be compared with the measured coherence length a_{ab} via Eq. (9).

Eq. (14) is clearly clarified in FIG 4 using mostly experimental information for a_{ab} , T_c and U_0 (values are given in Table I.). For Tl2201 no measured a_{ab} is found in the literature, therefore the estimated real space period is used (given in Table I.). The slope of the linear fit in FIG 4 precisely gives us k_B which nicely confirms Eq. (14). The underlying physics of HTSC seems to be reflected by Eq. (14): the equation couples the variables T_c , U_0 and a_{ab} .

We find correlation between the condensation energy U_0 and N : the larger U_0 is connected with smaller N (see also FIG 5). The stronger localization of the pair-condensate wave function seems to lead to larger IL condensation energy and hence to larger T_c . This is again an unexpected result, since the stronger localization of the Cooper pairs should increase the Coulomb

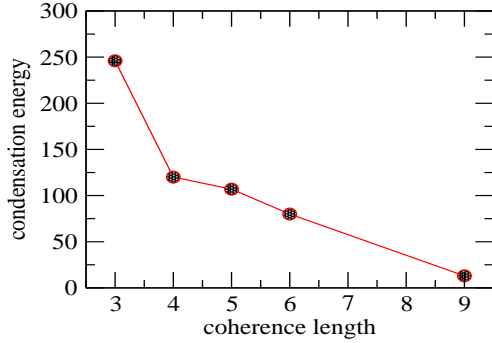


FIG. 5. The measured condensation energy (given in Table I., eV/u.c.) as a function of the calculated coherence length (a_0) using Eq. (15).

self-repulsion of the condensate and hence should suppress T_c . Note, however, that within a liquid-crystal-like COS the self-repulsion problem is not crucial. The hole-antihole Coulomb interactions are attractive, although cancelled by the intra-hole and intra-antihole repulsions (intra CuO_2 site repulsion,) and by the in-plane kinetic energy via Eq. (11).

The U_0 value for LSCO is measured for a slightly underdoped sample [53] therefore a somewhat higher U_0 might be obtained for the optimally doped material and hence smaller N and a_b can be calculated. Interestingly the most localized coherence area ($4a_0$) is provided by YBCO which is the less anisotropic material among HTSC cuprates (the resistivity ratio $a_b/a_c = 200$ [3]). The more anisotropic Hg1201 gives us somewhat weaker localization of the condensate wave-pocket for similar T_c . The comparison between various materials, however, is much more complicated. In general we can say that T_c is a function of the following parameters considered in this study: N , p , the IL distance d and ϵ_c . In section V III. we further analyse this complex behaviour of T_c focusing on the calculated IL dielectric constant ϵ_c . The calculated real-space periods given in Table I of the bilayer COS are in close agreement with the experimental coherence areas a_b which supports the validity of our basic Eq. (14).

The expression Eq. (14) leads to the very simple formula for the critical temperature

$$T_c(N; dg; d; \epsilon_c) = \frac{e^2}{4\epsilon_0 \epsilon_c k_B} \frac{X^2}{\sum_{n=1}^{N-1} \sum_{m=2}^{N-1} \frac{q_i^{(n)} q_j^{(m)}}{r_{ij}^{(n,m)}}} \quad (16)$$

where N_1 is the number of layers along the c -axis. When $N_1 \neq 1$, bulk T_c is calculated. T_c can also be calculated for thin films when N_1 is finite and ϵ_c can also be derived

$$\epsilon_c = \frac{e^2}{4\epsilon_0 k_B T_c} \frac{X^2}{\sum_{n=1}^{N-1} \sum_{m=2}^{N-1} \frac{q_i^{(n)} q_j^{(m)}}{r_{ij}^{(n,m)}}} \quad (17)$$

where a c -axis average of ϵ_c is computed when $N_1 \neq 1$.

TABLE I. The calculated real-space period of the pair condensate using the experimental condensation energies of various cuprates and Eq. (15).

	T_c (K)	$k_B T_c$ (meV)	U_0 (eV/u.c.)	N	a_b (a_0)
LSCO	32	2.5	13 ^a	10	5.8 ^e
Tl2201	85	7	80 ^a	7	
Hg1201	95	7.8	103 136 ^b	5 6	5 ^b
YBCO	92	7.5	246 ^c	4	3 4 ^f
Bi2212	89	7.3	107 ^d	6	4 8 ^g

U_0 is the measured condensation energy of various cuprates. ^a from [53], ^b from [54] and a_b from [55], ^c from [49], ^d from [24], ^e from [77], ^f from [22,50], ^g from [41,75], N is calculated according to Eq. (15) and a_b is the in-plane coherence length given in $a_0 = 3.88 \text{ \AA}$. The notations are as follows for the compounds: LSCO ($\text{La}_{1.85}\text{Sr}_{0.15}\text{CuO}_4$), Tl2201 ($\text{Tl}_2\text{Ba}_2\text{CuO}_6$), Hg1201 ($\text{HgBa}_2\text{CuO}_{4+}$), YBCO (YBa_2CuO_7) and Bi2212 is $\text{Bi}_2\text{Sr}_2\text{CaCu}_2\text{O}_{8+}$.

V I. RELATIONS TO THE SUPERCONDUCTING GAP AND PAIRING

Not useless to note again the correlation in Table I. between a_b and U_0 . There seems to be a correlation between the real-space localization of the Cooper wave-function and the SC energy gain U_0 . The real-space "shrinking" of the Cooper wave-function must directly be related to the enhancement of pairing. Within our model the primary source of increased pairing is the IL energy gain (Coulomb induced pairing).

Optimally doped YBCO/PBCO with decoupled layers show no HTSC ($T_c = 20 \text{ K}$) indicating that optimal carrier concentration within isolated layers leads to BCS superconductivity with low critical temperature. Setting in IL coupling (decreasing the thickness of the PBCO phase) T_c is enhanced due to the increase of IL coupling [3,6]. Further experimental studies on artificially layered materials, such as the measurement of a_b as a function of the thickness of the insulating phase PBCO should explain the importance of IL coupling in cuprates. The considerable increase in a_b as a function of IL decoupling (increase in PBCO thickness or decrease in YBCO thickness) would be a strong evidence for the model presented in sections IV -V I. Searching for such an article in the literature an interesting publication is found which reveals our expectation [68]. Extensive measurements of the upper critical field in (YBCO/PBCO) $_n$ superlattices indeed results in the increase of a_b as a function of decreased thickness of YBCO layers. a_b varies from $4.5a_0$ up to $8a_0$ when the thickness of the YBCO phase is decreased from 10 unit cells to 3. Unfortunately this article contains no measurements for 1-2 unit cell thick samples.

In FIG 6 we give the measured coherence length in YBCO/PBCO getting the data from ref. [68]. We predict the rapid increase of a_b for dielectrically isolated single layers of YBCO for one or two-unit-cell thick samples

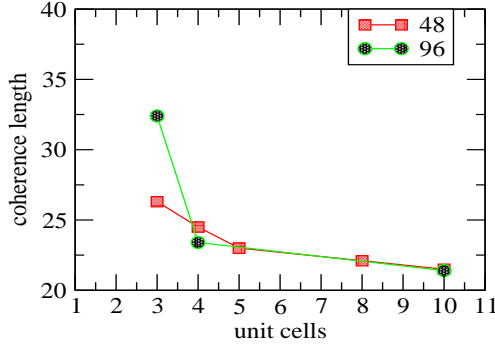


FIG. 6. The coherence length λ_{ab} (Å) as a function of the YBCO thickness (in unit cells) at fixed thickness of the barrier (insulating) layer PBCO (48 and 96 Å) reproduced from Table II. of ref. [68].

which is the remnant of purely BCS features. These striking results represent a strong evidence for the correlation between IL coupling and the coherence length λ_{ab} which is predicted by the model presented here. Strikingly, the contraction of the Cooper wave-function (the strengthening of pairing) is strongly coupled to the enhancement of IL Coulomb coupling.

As far as the microscopic nature of pairing is concerned, its relation to the SC gap should also be discussed. In the BCS theory the SC gap is related to the pair binding energy of the Cooper pairs [22]. However, keeping this scenario one can go easily into contradiction in HTSC. The increased gap ratio of cuprates $2 \approx 8k_B T_c$ [3,67] can not easily be understood as the enhancement of pair binding energy ("pairing glue"). Within our understanding of HTSC the more or less generic gap ratio $2 \approx 7-8k_B T_c$ [3,67] is rather a characteristic feature of the superconducting COS and does not directly correlate with the pair binding energy in the Cooper-pairs. The recently found doping-induced linear shift of the gap ratio in Bi2212 [24,67,69] supports the lack of extra "pairing glue" in HTSC cuprates. The gap ratio monotonically decreases with doping showing not any sign of critical properties at the optimal or critical doping level. If the enhancement of pairing played a decisive role in HTSC then the gap ratio should peak at T_c^m which is obviously not the case [70]. The more or less constant value of the maximum gap ratio $2 \approx 7-9k_B T_c$ in various cuprates [3] is also not consistent with the "pairing glue" scenario. 2 should vary system by system as a function of T_c if pairing enhanced with the increase of T_c . However, systems with low $T_c \approx 40$ K, such as the prototypical HTSC material $\text{La}_{2-x}\text{Sr}_x\text{CuO}_4$ (LSCO) provides a relatively large gap as well ($2 \approx 7.7k_B T_c$) [3,69]. Others measure a relatively small gap of $2 \approx 5k_B T_c$ for YBCO [72]. Anyhow, the interpretation of the measured gaps and its relation to pairing is still a matter of debate in HTSC [71,73]. We also attribute the pseudogap phenomenon of cuprates to the characteristic feature of the

Wigner crystal-like COS of the normal state. This field is, however, obviously beyond the scope of the present study.

VII. THE DIELECTRIC CONSTANT ϵ_c WITHIN THE BCS LIMIT

The model outlined in the previous section allows us to estimate the static dielectric constant ϵ_c for various cuprates. First we give the brief derivation of the formula starting from the BCS equation for the gap [22],

$$k_{BCS} k_B T_c = \Delta(0); \quad (18)$$

where k_B is the Boltzmann constant and the gap ratio $k_{BCS} \approx 3.53$ for normal superconductors at weak-coupling limit [22]. The BCS estimate of the condensation energy (the energy gain in the SC state) is proportional, however to Δ^2 , therefore we can use the following expression [22],

$$E_{\text{cond}} = \frac{1}{2} N(0) \Delta(0)^2 = \frac{1}{2} N(0) k_{BCS}^2 k_B^2 T_c^2; \quad (19)$$

where $N(0)$ is the density of states at the Fermi surface [22]. We recall now Eq. (13),

$$E_{\text{cond}} - E_c^{\text{IL}} = \frac{e^2}{4} \sum_{n=1}^{\infty} \sum_{m=2}^{\infty} \frac{X^2}{\epsilon_{ij}^{(n,m)}} \frac{q_i^{(n)} q_j^{(m)}}{r_{ij}^{(n,m)}}; \quad (20)$$

from which ϵ_c can be derived,

$$\epsilon_c = \frac{e^2}{4 E_{\text{cond}}} \sum_{n=1}^{\infty} \sum_{m=2}^{\infty} \frac{X^2}{\epsilon_{ij}^{(n,m)}} \frac{q_i^{(n)} q_j^{(m)}}{r_{ij}^{(n,m)}}; \quad (21)$$

Using Eq. (19) E_{cond} can be substituted into Eq. (21) leading to a new expression,

$$\epsilon_c = \frac{2e^2}{4 N(0) k_{BCS}^2 k_B^2 T_c^2} \sum_{n=1}^{\infty} \sum_{m=2}^{\infty} \frac{X^2}{\epsilon_{ij}^{(n,m)}} \frac{q_i^{(n)} q_j^{(m)}}{r_{ij}^{(n,m)}}; \quad (22)$$

$N(0)$ can be obtained from first-principles calculations or from specific-heat measurements. $N(0)$ is connected with the Sommerfeld constant in the low-temperature electronic specific heat by the relation

$$N(0) = \frac{2}{3} k_B^2 (1 + \gamma)^{-1}; \quad (23)$$

is a coupling constant due to strong electron-phonon renormalization. γ can be obtained from specific heat measurements [3]

$$1.43 \gamma = \gamma_C = T_c; \quad (24)$$

where γ is usually given in $[mJ/molK^2]$ therefore $2N(0)^{-2}$ must be used for the coherence area of $\frac{2}{\lambda_{ab}}$ (twice

for the bilayer). Finally we get the expression for the static c-axis dielectric constant

$$\epsilon_c = \frac{e^2 (1 + \epsilon_\infty)}{6 \epsilon_0 k_B^2 N^2 T_c^2} \sum_{n=1}^{\infty} \sum_{m=2}^{\infty} \sum_{ij} \frac{X_{ij}^2 X_{ij}^4 X_{ij}}{X_{ij}^{(n,m)}} \frac{q_i^{(n)} q_j^{(m)}}{r_{ij}^{(n,m)}}; \quad (25)$$

The only unknown parameter in Eq. (25) is ϵ_∞ which is in the range of $\epsilon_\infty = 1 - 2$ when strong electron-phonon coupling is assumed [3].

We use later on in the discussion section this expression to calculate ϵ_c within the BCS limit for various cuprates comparing with the experimental dielectric constants.

V III. THE CALCULATED DIELECTRIC CONSTANT

The calculation of the c-axis dielectric constants ϵ_c might provide further evidences for Eq. (14) when compared with the measured values [36,58,65]. In Table II we have calculated the static dielectric function ϵ_c using Eqs. (25) and (17) and compared with the experimental impedance measurements [59]. ϵ_c can also be extracted from the c-axis optical measurements using the relation [19,49]

$$\epsilon_c = \frac{c}{v_p^2}; \quad (26)$$

where c , v_p and ϵ_c are the speed of light, c-axis plasma frequency and the c-axis penetration depth.

In other cases only the ϵ_c of certain elements of the ion-core spacer is available such as e.g. BaO in Hg1201 and in YBCO. For the prototypical cuprate LSCO we get the value of $\epsilon_c = 27.3$ which is comparable with the experimental value of 23 [58] using $N = 7$ which corresponds to $6a_0 = 23.4\text{\AA}$ ($a_b = 20 - 30\text{\AA}$ [77]).

The overall good agreement of the calculated ϵ_c with the measurements is due to our finding that the IL charging energy is surprisingly in the range of $k_B T_c$ when the real space period N is reasonably chosen. Although we have no clear cut evidence for Eq. (14) we do not think that the agreement of various calculated properties with the measurements is accidental. In the rest of the article we collect further evidences which validates Eq. (14).

Multilayer and pressure effects on T_c can also be discussed in terms of in-plane and out-of-plane localization of the hole charge. In multilayer systems E_c^{IL} is composed of intra- and inter-block contributions. We use the notation block for the multilayer parts CaCuO_4 , $\text{Ca}_2\text{Cu}_3\text{O}_6$, etc. Eq. (13) can then be modified for multilayer cuprates as follows,

$$E_{\text{cond}} = E_c^{IL; \text{intra}} + E_c^{IL; \text{inter}}; \quad (27)$$

where

$$E_c^{IL; \text{intra}} = (1 - 1/N) E_c^{IL} (d_{\text{intra}}; \text{intra}); \quad (28)$$

TABLE II. The calculated dielectric constant ϵ_c using Eqs. (25) and (17) in various cuprates as a function of the real-space period N of the charge ordered state.

	$d(\text{\AA})$	$T_c(\text{K})$	N	$\epsilon_c(\text{A})$	$\epsilon_c(\text{B})$	ϵ_c^{exp}
CaCuO ₂ ^b	4.64	110	5	96.7	80.8	
CaCuO ₂	3.19	89	8	123.5	83.5	
			9	94.9	64.1	
LSCO	6.65	39	6	39.9	27.9	23; 13.5 ^c
			7	39.2	27.3	
			8	16.3	11.3	
Hg1201	9.5	95	5	17.7	27.6	34 ^d
Hg- (10 GPa)	8.5	105	5	15.9	27.6	
Hg- (20 GPa)	8.2	120	5	12.6	25.0	
Tl2201	11.6	85	4	13.5	8.7	11.3 ^e
			5	41.6	26.8	
			6	20.1	13.0	
			7	12.5	8.0	
Bi2201	12.2	20	4	214.5	32.6	40 ^g
			5	729.3	110.8	
			6	66.6	10.1	
YBCO	8.5 ^h	93	4	27.5	19.4	34 ^f ; 23.6 ^j
			5	44.1	31.1	
LSCO ⁱ	6.65	51.5	7	21.6	20.2	

where N is the real space period of the characteristic square lattice ($N_{ab} = a_0 + 1$), the bold faced values are those which account the best for comparison with experiment and are in accordance with the results of Table I. dq is the charge separation in the charge ordered state, d is the inter-layer distance in \AA [14], T_c is the experimental critical temperature. $\epsilon_c(\text{A})$ is from Eq. (25), $\epsilon_c(\text{B})$ is from Eq. (17). ^b $\text{Ca}_{0.3}\text{Sr}_{0.7}\text{CuO}_2$ [61], ^c [58], or from reactivity measurements using Eq. (26), $v_p = 55\text{cm}^{-1}$ [79], $\epsilon_c = 3\text{m}$ [62], ^d experimental ϵ_c^{exp} values are taken from Am. Inst. of Phys. Handbook, McGraw-Hill, Ed. D. E. Gray (1982), the ϵ_c value of the ionic-background (Hg1201: BaO, Tl2201: Tl₂O₅), The pressure dependent T_c values and IL distance data are taken from [66,74], ^e from [19], ^g from [36], ^h for YBCO the reduced IL $d = 8.5\text{\AA}$ is used instead of the c-axis lattice constant (inter-bilayer block distance), ^f from [65], ⁱ from [80], ^j from reactivity measurements: $v_p = 60\text{cm}^{-1}$ [79], $\epsilon_c = 0.9\text{m}$ [37], ϵ_c can be deduced using Eq. (26). The notations are as follows for the compounds: LSCO ($\text{La}_{1.85}\text{Sr}_{0.15}\text{CuO}_4$), Hg1201 ($\text{HgBa}_2\text{CuO}_{4+}$), Tl2201 ($\text{Tl}_2\text{Ba}_2\text{CuO}_6$), Bi2201 ($\text{Bi}_2\text{Sr}_2\text{CuO}_6$) and YBCO (YBa_2CuO_7).

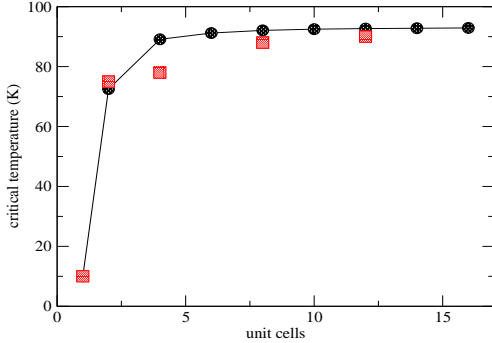


FIG. 7. The critical temperature T_c (K, Eqs. (14)–(17)) vs. the number of unit cells along the c -axis in YBCO using the 4 × 4 model. Circles and squares correspond to the calculated and experimental values [6].

l denotes the number of layers.

Therefore, intra-block charging energy further enhances T_c on top of the corresponding single-layer inter-block value. YBCO is a peculiar example of cuprates in which HTSC is purely coming from inter-block coupling as it was explained on the basis of $\text{YBa}_2\text{Cu}_3\text{O}_{7-x} \Rightarrow \text{PrBa}_2\text{Cu}_3\text{O}_{7-x}$ superlattice structures [3]. In YBCO the $\text{Y}(\text{CuO}_2)_2$ bilayer alone does not show HTSC when isolated from each other in artificially layered materials ($T_c \approx 20\text{K}$). The dependence of T_c in YBCO on the number of unit cells along the c -axis is calculated using Eq. (16) and the results are depicted on FIG. 7. The experimental points [6] are relatively well reproduced indicating that 5 unit cell thick thin film is already the representative of the bulk properties of cuprates.

It is worth mentioning the intercalation experiment on Bi2212 [4]. Intercalation of I or organic molecules into the $(\text{BiO})_2(\text{SrO})_2$ layers of Bi2212 results in no significant change in T_c . Basically inter-layer intercalation is introduced to reduce interlayer coupling (test of inter-layer theory, ILT) and to enhance anisotropy in SC properties. Using In deposition technique, ultrathin films of Bi-Sr-Ca-Cu-O (Bi2212) have been synthesized [78]. The few-unit-cell-thick samples show HTSC similar to that of the bulk material independently of the film thickness. These results present great challenge to ILT [11] and support low-dimensional SC theories.

In the light of the NN model, however, it is not surprising that in Bi2212 the nearly isolated bilayers are superconductors. The single layer material Bi2201 ($\text{Bi}_2\text{Sr}_2\text{CuO}_6$) gives very low T_c ($\approx 20\text{K}$) [64], which indicates that the dielectrics $(\text{BiO})_2(\text{SrO})_2$ strongly reduces IL coupling, indeed the estimated ϵ_c is quite large (Table II) which is attributed to the weakly interacting $(\text{BiO})_2$ bilayer (the $\text{BiO}-\text{BiO}$ distance is 3.7\AA [4]). Dielectric constant measurements [57] and the obtained small plasma frequency using c -axis optical measurements ($\approx 5\text{cm}^{-1}$) [79] in Bi compounds also provide relatively large dielectric constants in accordance

with our calculations. The extremely large conduction anisotropy $\sim 10^6$ found in Bi-based cuprates also supports these findings [3]. Nearest-neighbouring Cu-O planes in Bi compounds are nearly insulated [65]. Therefore, in the multilayer Bi compounds bilayer and trilayer blocks are responsible for the high- T_c , inter-block coupling is negligible. The multilayer Bi compounds provide then an example for pure intra-block HTSC. In these materials the multilayer blocks are dielectrically isolated. However, in the most of the cuprates T_c is enhanced both via intra- and inter-block effects. An important consequence of the bilayer NN model is that isolated single layers do not show HTSC, coupling to next-nearest CuO_2 plane is essential in HTSC. It is possible then to estimate ϵ_c for the bilayer block, since $E_c^{\text{IL}; \text{inter}} = 0$ in the Bi compounds in Eq. (27). In the hypothetical bilayer system in Table II ($\text{Ca}(\text{CuO}_2)_2$; $d = 3.19\text{\AA}$; $T_c = 89\text{K}$), which is the building block of bilayer cuprates, we find the value of $N = 8$ accounting for realistic ϵ_c . $N = 8$ is in accordance with the measured relatively "large" coherence length of $a_b \approx 27\text{\AA}$ ($(N-1)a_0 = 7a_0 \approx 27.3\text{\AA}$) [75].

Also, upon pressure (p) the inter-layer spacing decreases, which increases E_c^{IL} without the increase of the hole content. Saturation of $T_c(p)$ is reached simply when increasing IL steric repulsion starts to destabilize the system. In systems, such as YBCO or LSCO, negative or no pressure dependence of T_c is found [3] due to the short Cu-O apical distance ($d_{\text{CuO}} \approx 2.4\text{\AA}$) which leads to already steric repulsion at ambient pressure and to the weakening of HTSC. In these systems the net gain in charging energy is not enough to overcome steric repulsions at high pressures.

With these results, we are now in a position to reach the conclusion that the NN model can readily account for at least certain physical properties of multilayer cuprates, such as pressure, doping and multilayer dependence of T_c . Furthermore it is possible to make some estimations on the upper limit of T_c using Eq. (17) for T_c . Assuming relatively small $\epsilon_c \approx 10$ and short inter-layer spacing $d = 7.0\text{\AA}$ we get the value of $T_c = 333\text{K}$ for a strongly localized electron pair with 5×5 coherence area. Of course, we have no clear cut knowledge at this moment on how the pair condensate wave-function spreads upon varying ϵ_c and d . Effective localization of the Cooper-pair wave-pocket could lead, however, to room temperature superconductivity under proper structural and dielectric conditions if the model presented above is applicable.

According to the stripe scenario, the charge ordered state of the coherence area can also be seen in many cuprates as one-dimensional stripe order or charge density waves [43]. The striped antiferromagnetic order found in LSCO by magnetic neutron scattering experiments [42] also implies a spin-density of periodicity $\approx 8a$ a remnant of the coherence area. The incommensurate "checkerboard" patterns seen with a spatial periodicity of $\approx 8a_0$ in the vortex core of Bi2212 obtained by scanning tunneling microscopy [41] is also consistent with our

$N \times N$ hole-anti-hole charge ordered state where $N = 8$ to 9 in BSSCO.

Finally we mention the recent results of Bozovic et al. [80] obtained for LSCO thin films under epitaxial strain. They reached the record $T_c = 51.5\text{K}$ for 15-unit-cell thick

film of LSCO on LaSrAlO_4 substrate. The small variation of the ab- or c-axis lattice constants in our model accounts for only 1–2 K increase in T_c . We explain the more than 10 K enhancement of T_c with the decrease of ϵ_c (Table II) under the conditions they used (O_3 annealing, epitaxial strain provided by the substrate).

IX. CONCLUSION

In this paper we studied the pair condensation and confinement of the hole-content on a CuO_2 superlattice layer as a function of inter-layer distance and dielectric permittivity of the charge reservoir.

The assumption of a 2D, 3D quantum phase transition of the hole-content at T_c in HTSC materials is thought to be an important general feature of pair-condensation and is supported by c-axis optical measurements and by first-principles calculations. Our proposal is that the c-axis charge dynamics of the hole-content contributes significantly to the condensation energy below T_c . We find that the inter-layer capacitance is temperature dependent in cuprates and therefore the drop of the c-axis dielectric constant can be seen below T_c . This is what leads to then the stabilization of the superconducting state vs. the normal state.

We have found that a pair condensate can be distributed on a $N \times N$ square lattice layer in such a way that the lattice sites are filled by $q = [0; 0.16e]$ condensed charge alternatively depending on the hole(+q)-anti-hole(-q) charge separation dq . In this way a charge ordered state of the pair-condensate occurs with a "checkerboard" like pattern seen recently by experiment [41]. The phase separation of hole-electron pairs (hole-anti-hole pairs) in this model is stabilized electrostatically. The maximum charge separation is $dq = 0.32e$, if the optimal hole content $p_0 = 0.16e$.

In the adjacent layer the electron-hole pairs are distributed in a complementary way (charge asymmetry) in order to maximize the inter-layer charging energy. Holes on one plane are covered by anti-holes on the other, and vice versa. In this way we derived a charge ordered $N \times N$ bilayer-hole model of the superconducting state with inter-layer charge antisymmetry which directly leads to inter-layer Coulomb energy gain in the superconducting state. The IL charge asymmetry could directly be tested experimentally using e.g. two-cell-thick

thin SC films, and the "checkerboard" STM images of both sides of the thin film could be measured. The complementary "checkerboard" charge pattern would reveal our expectations.

The superlattice nature of the pair condensate is directly related to the smallest size of the condensate wave-pocket which is remarkably comparable with the measured in-plane coherence length of $a_b = 10-20\text{\AA}$ ($4a_0 = 15.6\text{\AA}$) of single cuprates, where $a_0 = 3.9\text{\AA}$ is the in-plane lattice constant. The coherence area of the Cooper-pair wave-function in cuprates is strongly localized, which is due to inter-layer charging effects.

The bilayer model with 4e boson charge naturally implies the mass enhancement of $m = 4m_e$ in accordance with measurements. The calculated inter-layer charging energy is in the range of the experimental condensation energy for the bilayer-hole system.

The static dielectric constant ϵ_c is calculated for a couple of cuprates and compared with the available experimental measurements. The general agreement is quite good indicating that the pure inter-layer electrostatic model leads to proper description of the static dielectric response of these layered materials.

The basic microscopic mechanism of HTSC is to be understood within the BCS-Eliashberg theory. The limiting critical temperature for BCS-type superconductor is around 20K as it was found for cuprates with nearly isolated CuO_2 layers (BSCCO, YBCO/PBCO superlattices etc.). The detailed study of this model showed that the inter-layer charging energy is proportional to the thermal motion at T_c , if the c-axis dielectric constant ϵ_c and the coherence area is appropriately chosen. The correlation between the coherence area a_b and inter-layer coupling is predicted by our model. The stronger IL coupling leads to smaller a_b . This relation is evidenced by the measurements of a_b in YBCO/PBCO films with varying YBCO thickness.

If the physical picture derived from our model is correct, it should be a guide for further experimental studies aiming to improve SC in cuprates or in other materials. This can be done by tuning the IL distance and ϵ_c (increasing the polarizability of the dielectric, hence decreasing ϵ_c) in these materials. The application of this model to other class of HTSC materials, such as fullerides or MgB_2 is expected to be also effective.

X. ACKNOWLEDGEMENT

It is a privilege to thank M. Menyhárd for his continuous support. I greatly indebted to E. Shernan for reading the

manuscript carefully and for the helpful informations. I would also like to thank for the helpful discussions with T. G. Kovacs. This work is supported by the OTKA grant MFA-42/2002 from the Hungarian Academy of Sciences

-
- [1] Q. Xiong, Y. Y. Xue, Y. Cao, F. Chen, Y. Y. Sun, J. Gibson, and C. W. Chu, *Phys. Rev. B* 50, 10346 (1994)
- [2] J. E. Hirsch, *Science* 295, 2226. (2002)
- [3] N. M. P. Lakida, *High-Temperature Superconductivity*, Springer, 1995
- [4] J. Choy et al., *Science* 280, 1589. (1998), X.-D. Xiang, et al., *Nature* 348, 145. (1990)
- [5] D. N. Basov et al., *Science* 283, 49. (1999)
- [6] Q. Li, et al., *Phys. Rev. Lett.* 64, 3086. (1990)
- [7] G. Balestrino et al., *Phys. Rev. B* 58, 8925. (1998)
- [8] T. Terashima, et al., *Phys. Rev. Lett.* 67, 1362. (1991)
- [9] G. Balestrino et al., *Phys. Rev. Lett.* 89, 156402-1 (2002)
- [10] P. W. Anderson, *The Theory of Superconductivity in the High-T_c Cuprate Superconductors*, Princeton Univ. Press, 1997
- [11] P. W. Anderson, *Physica C* 341-348, 9. (2000), *cond-mat/0201429*
- [12] T. Schneider, *cond-mat/0110173*, T. Schneider, H. Keller, *Phys. Rev. Lett.* 86, 4899. (2001)
- [13] J. M. Wheatley, T. C. Hsu, P. W. Anderson, *Nature* 333, 121. (1988)
- [14] D. R. Harshman, A. P. Mills, *Phys. Rev. B* 45, 10684. (1992), and references therein
- [15] Z. Tesanovic, *Phys. Rev. B* 36, 2364. (1987)
- [16] A. K. Rajagopal, S. D. Mahanti, *Phys. Rev. B* 44, 10210. (1991), S. S. Jha, A. K. Rajagopal, *Phys. Rev. B* 55, 15248. (1997)
- [17] X.-D. Xiang, et al., *Phys. Rev. Lett.* 68, 530. (1992)
- [18] J. Ihm and B. D. Yu, *Phys. Rev. B* 39, 4760. (1989)
- [19] A. A. Tsvetkov et al., *Nature*, 395, 360. (1998)
- [20] H. J. A. M. olegraaf, C. Presura, D. van der Marel, P. H. Kes, M. Li, *Science* 295, 2239. (2002), D. van der Marel, A. Tsvetkov, M. G. Rueninger, H. J. A. M. olegraaf, *Physica C* 341-348, 1531. (2000)
- [21] J. E. Hirsch, *Physica C* 199, 305. (1992)
- [22] M. Tinkham, *Introduction to Superconductivity*, McGraw-Hill, Inc. New York, 1996
- [23] J. B. Torrance et al., *Phys. Rev. Lett.* 61, 1127. (1988), H. Zhang and H. Sato, *Phys. Rev. Lett.* 70, 1697. (1993)
- [24] J. L. Tallon, et al., *Phys. Rev. B* 51, 12911. (1995)
- [25] K. Tamasku, Y. Nakamura, S. Uchida, *Phys. Rev. Lett.* 69, 1455. (1992)
- [26] S. Tajima, et al., *Phys. Rev. B* 48, 16164. (1993)
- [27] A. S. Katz, et al., *Phys. Rev. B* 61, 5930. (2000)
- [28] D. N. Basov, et al., *Phys. Rev. B* 63, 134514. (2001)
- [29] T. Motohashi, et al., *Phys. Rev. B* 61, 9269. (2000)
- [30] W. E. Pickett, *Rev. Mod. Phys.* 61, 433. (1989)
- [31] R. P. Gupta, M. Gupta, *Phys. Rev. B* 21, 15617. (1995)
- [32] P. Sule, C. Ambrosch-Drahl, H. Auer, E. Y. Sherman, *cond-mat/0109089*
- [33] Y. Ando, A. N. Lavrov, S. Komiyama, K. Segawa, X. F. Sun, *cond-mat/0104163*
- [34] K. Semba, A. Matsuda, *Phys. Rev. Lett.* 86, 496. (2001)
- [35] A. Yamamoto, W. Hu, S. Tajima, *Phys. Rev. B* 63, 24504. (2001)
- [36] H. Kitano, T. Hanaguri, A. Mada, *Phys. Rev. B* 57, 10946. (1998), C. C. Homes, et al., *Science*, 293, 673. (2001)
- [37] H. Kitano et al., *Phys. Rev. B* 51, 1401. (1995)
- [38] T. Fujii, et al., *cond-mat/0205121*, L. He, et al., *cond-mat/0110166*, W. Si, et al., *cond-mat/0205153*
- [39] R. Friedberg, H. S. Zhao, *Phys. Rev. B* 44, 2297. (1991), *Phys. Rev. B* 39, 11482. (1989)
- [40] M. Voja, Y. Zhang, S. Sachdev, *Phys. Rev. B* 62, 6701. (2000)
- [41] J. E. Hoffman et al., *Science* 295, 466. (2002)
- [42] B. Lake, et al., *Nature* 415, 299. (2002)
- [43] C. Howald, et al., *cond-mat/0208442*
- [44] E. Dagotto, et al., *cond-mat/0209689*
- [45] M. Voja, *cond-mat/0204284*
- [46] E. Dagotto, *Rev. Mod. Phys.* 66, 763. (1994)
- [47] S. Stinzingen, Z. Zwebger, *Phys. Rev. B* 56, 9004. (1997)
- [48] M. Di Stasio, K. A. Müller, L. Pietronero, *Phys. Rev. Lett.* 64, 2827. (1990), and references therein
- [49] P. W. Anderson, *Science*, 279, 1196. (1998)
- [50] U. Welp, et al., *Phys. Rev. Lett.* 62, 1908. (1989)
- [51] L. K. Nussli-Eibaum et al., *Phys. Rev. Lett.* 62, 217. (1989)
- [52] J. L. Tallon et al., *cond-mat/0211048*,
- [53] J. W. Loram et al., *J. Phys. Chem. Solids*, 62, 59. (2001) and references therein
- [54] B. Billon et al., *Phys. Rev. B* 56, 10824. (1997)
- [55] J. R. Thompson, et al., *Phys. Rev. B* 54, 7505. (1996)
- [56] C. Kittel, *Quantum Theory of Solids*, Wiley & Sons, New York, (1987)
- [57] K. B. R. Vam, et al., *Appl. Phys. Lett.* 55, 75. (1989)
- [58] Optical reflectance measurements indicate an in-plane dielectric constant of 5-6 at low frequencies: D. Reagor et al., *Phys. Rev. Lett.* 62, 2048. (1989)
- [59] T. Takayanagi, M. Kogure, I. Terasaki, *cond-mat/0108483*, and references therein, I. Terasaki, T. Mizuno, K. Inagaki, Y. Yoshino, *cond-mat/0204537*
- [60] R. M. Hazen, *Crystal Structures of High Temperature Superconductors*, in *Physical Properties of High Temperature Superconductors*, Ed. D. M. Ginsberg, (1990)
- [61] M. Azuma et al., *Nature (London)* 356, 775. (1992)
- [62] J. R. Kirtley, et al., *Phys. Rev. Lett.* 81, 2140. (1998)
- [63] P. Nozières, D. Pines, *The Theory of Quantum Liquids*, Perseus Books, 1999
- [64] Z. Konstantinovic, et al., *Phys. Rev. B* 66, 20503. (2002)
- [65] D. A. Rios, H. Beck, *Phys. Rev. B* 43, 344. (1991)
- [66] D. L. Novikov et al., *Phys. Rev. B* 54, 1313. (1996)
- [67] T. Timusk, B. Statt, *Rep. Prog. Phys.* 62, 91. (1999)
- [68] H. C. Yang, L. M. Wang, H. E. Homg, *Phys. Rev. B* 59, 8956. (1999)
- [69] K. C. Hewitt, J. C. Irwin, *Phys. Rev. B* 66, 054516, (2002), *cond-mat/0012413*
- [70] C. Panagopoulos, T. Xiang, *Phys. Rev. Lett.* 81, 2336. (1998)
- [71] M. Opel, et al., *Phys. Rev. B* 61, 9752. (2000)

- [72] J. Demsar, B. Podobnik, V. V. Kabanov, Th. Wolf, D. Mihailovic, Phys. Rev. Lett. 82, 4918. (1999)
- [73] D. Mihailovic, V. V. Kabanov, K. A. Müller, Europhys. Lett. 57, 254. (2002)
- [74] L. Gao, et al, Phys. Rev. B 50, 4260. (1994)
- [75] I. Matsubara, et al, Phys. Rev. B 45, 7414. (1992)
- [76] R. Kleiner, et al, Phys. Rev. Lett. 68, 2394. (1992)
- [77] See e.g. Physical Properties of High Temperature Superconductors, Ed. D. M. Ginsberg, (1989)
- [78] K. Saito, M. Kaise, Phys. Rev. B 57, 11786. (1998)
- [79] S. Das Sarma, E. H. Hwang, Phys. Rev. Lett. 80, 4753. (1998)
- [80] I. Bozovic et al, Phys. Rev. Lett. 89, 107001. (2002)